

Degradation of reinforced concrete structures under atmospheric corrosion

A. Millard

CEA/DEN/DM2S/SEMT/LM2S, Saclay, France

V. Leyre

CUST, Aubière, France

V. L'Hostis

CEA/DEN/DPC/SCCME/LECBA, Saclay, France

ABSTRACT: For the study of long term atmospheric corrosion of rebars embedded in concrete, a reactive transport model has been developed, considering the kinetic of oxygen diffusion through the system and its consumption at the metal/dense product layer interface as a function of concrete water saturation degree. Corrosion products growth can then be simulated and used as input to a mechanical model capable of predicting the damage induced by corrosion. This multi-physics model has been implemented and first applied to a simple bi-dimensional reinforced concrete slab. Then the model has been applied to a three-dimensional beam, inspired from chloride corrosion experiments performed at LMDC (INSA Toulouse). Special attention has been given to the outer environmental conditions, in order to investigate their role in the corrosion degradation phase.

1 INTRODUCTION

1.1 *General context of the study*

Cracking of concrete due to corrosion is a very common pathology that can be observed on various structures. Corrosion is initiated by the penetration of chlorides or of carbon dioxide in most cases. As reinforced concrete is a common material used in the nuclear industry for the construction of power plants and nuclear waste storage facilities, the degradation of infrastructures has to be mechanically understood and modeled. In this context, the CIMETAL research program has been launched by the French Commissariat à l'Energie Atomique (CEA), for the prediction of the evolution of cement/metallic material systems in an open unsaturated environment. It deals first with interactive studies dedicated to short term experimentations, then with modelling to predict the corrosion and the mechanical behavior of objects for several hundred years, and finally with validation of some hypotheses by analyses of old corrosion systems (L'Hostis et al. 2008).

1.2 *Previous modeling work*

The expansive nature of the corrosion products which are formed at the rebars surface cause the de-

velopment of mechanical tensile stresses in the concrete, as well as confining stresses on the rebars. When the tensile stresses reach the concrete traction strength, some cracks develop first around the rebars, and then further on, according to the rebars arrangement (position in the structure, number of rebars, cover, etc), some through cracks are formed, which can be observed at the concrete surface. The numerical modelling of concrete cracking due to corrosion, has been first achieved by means of the CORDOBA model which consists in using a damage model, such as the Mazars' model (Mazars 1984), for the concrete, together with an interface element for the corrosion products layer (Millard et al. 2004). Starting with the onset of the active corrosion phase, a given corrosion rate, possibly variable with time, is used to evaluate the growth of the corrosion layer thickness. This model has proved capable of reproducing the cracks development as well as the final crack pattern observed in experiments on centimetric slabs containing a reinforcement (Nguyen et al. 2006). The corrosion was artificially accelerated using a prescribed electric current. The comparison between the observed and predicted cracks patterns is presented on figure 1.

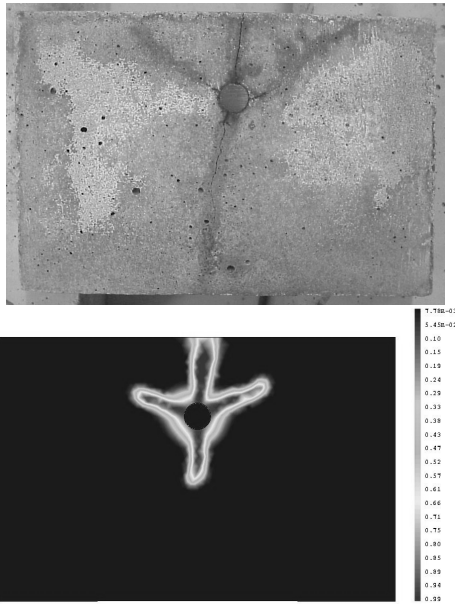


Figure 1. Comparison of cracks pattern, after 40 hours of accelerated corrosion, between experiment (top) and prediction (bottom).

In the case of corrosion due to carbonation under atmospheric conditions, the corrosion rate can be estimated in the cases where the carbonation depth can be measured on a given corroded reinforced concrete structure, assuming a mainly diffusive process. However, in the more general case, the corrosion rate depends on the environmental conditions and on the transfer properties of concrete and should therefore be predicted. The development of such a model is exposed in the following paragraph.

2 ATMOSPHERIC CORROSION MODEL

2.1 Model hypothesis

The following model has been proposed by Huet et al. (2005), Chitty et al. (2008). In this model, the corrosion reactions take place at the interface between the iron and the already formed corrosion products. These reactions are on one hand the iron oxidation, with OH⁻ ions, and on the other hand, the oxygen reduction. It is assumed here that the iron oxidation rate is much greater than the oxygen reduction rate. Therefore, the corrosion rate is controlled by the amount of oxygen which depends on the diffusion through the concrete and the corrosion products, and on the chemical reaction kinetic. It also depends on the amount of water which is present in the porous material surrounding the rebar, and which can be characterized by the saturation degree $S_{r,CPD}$. The following expression of the corrosion rate has thus been adopted:

$$v_{corr}(x,t) = \frac{4}{3} \frac{M_{Fe}}{\rho_{Fe}} k \varphi S_{r,CPD}(x,t) C_{O_2}(x,t) \quad (1)$$

where x corresponds to any point of the rust-iron interface, M_{Fe} denotes the molar mass of iron, ρ_{Fe} its density, k the reaction kinetic constant, φ the corro-

sion products porosity and C_{O_2} the oxygen concentration. The coefficient $4/3$ is linked to the stoichiometric coefficients of the reaction which involves 3 oxygen moles for 4 iron moles.

The determination of the corrosion rate thus requires the calculation of the saturation degree, by means of a drying model, as well as the oxygen concentration by means of a diffusion model.

2.2 Drying model

The drying model enables to determine the time history of the saturation degree in the concrete as well as in the corrosion products. In the more general case, the water transport in a porous material can be in liquid and gaseous phases. Here, it is assumed for simplicity that the dominant transport mode is the liquid one, under a liquid pressure gradient, while the gas remains at atmospheric pressure. Assuming a constant porosity as well as a constant water density ρ_l , the water mass conservation can be written as following :

$$\rho_l \varphi \frac{\partial S_r}{\partial t} + \text{div } w_l = 0 \quad (2)$$

where the water flux w_l is given by the generalized Darcy's law :

$$w_l = - \frac{K \rho_l}{\eta} k_{rl}(S_r) \nabla p_l(S_r) \quad (3)$$

In this equation, K is the intrinsic permeability, η the dynamic water viscosity, p_l the liquid water pressure, and k_{rl} the relative liquid permeability, which depends on the saturation degree. The pressure gradient can be related to the saturation degree by using the capillary pressure curve. Here, the classical Van Genuchten's model (1980) has been used to approximate the capillary pressure curve as well as the liquid relative permeability:

$$p_c(S_r) = \beta (S_r^\alpha - 1)^{1 - \frac{1}{\alpha}} \quad (4)$$

$$k_{rl}(S_r) = \sqrt{S_r} \left\{ 1 - (1 - S_r^\alpha)^{1/\alpha} \right\}^2 \quad (5)$$

where α and β are fitting parameters.

Finally, combining these equations leads to a non linear partial differential equation governing the saturation degree.

2.3 Oxygen diffusion model

The transport of oxygen in the concrete and in the corrosion products occurs in gaseous as well as liquid phase. For simplicity, it has been assumed here that the porous medium is not fully saturated and therefore, the transport of oxygen in gaseous form is the dominant one. It obeys a Fick's law such as :

$$\frac{\partial C_{O_2}}{\partial t} = \text{div}(D_{O_2} \nabla C_{O_2}) - k' C_{O_2} \quad (6)$$

D_{O_2} is the coefficient of diffusion of oxygen in gaseous phase. Because of the lack of data, it has been taken identical for the rust and for the concrete. It depends on the saturation degree according to the Papadakis' law (1991):

$$D_{O_2} = K(1 - S_r)^n \quad (7)$$

In this expression, K and n are constants which depend, among other parameters, on the water/cement ratio of the concrete. The diffusion coefficient varies rapidly for high saturation degrees, and slowly for saturation degree below 60%.

The reaction of oxygen at the interface between the rust and the iron is responsible for the consumption term which appears in the right-hand side of equation (6). k' is the corresponding reaction rate, which is related to the reaction kinetic constant through the following equation:

$$k' = k S_r \varphi \quad (8)$$

In case of full saturation, the model should be extended to include the diffusion of oxygen in the liquid phase.

For any time, the above coupled equations are solved in the Cast3M computer code (Verpeaux et al. 1989) together with the classical mechanical ones.

3 APPLICATION TO A REINFORCED CONCRETE SLAB

3.1 Studied slab and model set-up

The above described model has been first applied to a simple structure, in a bi-dimensional case, in order to check its adequacy with experimental observations. The studied structure has been inspired by the slabs originally used to investigate the formation of the corrosion cracks pattern (Nguyen et al. 2007), as shown on figure 1. The concrete section is 50cmx50cm and it contains only one rebar cross-section of 18mm diameter. An initial rust layer of 0.5mm thickness has been assumed. For symmetry reasons, only one half of the slab has been modelled, the symmetry line being AB (see Fig. 1). On this boundary normal fluxes as well as normal displacements are set to zero. Boundaries BC and CD are supposed to be impervious to water and oxygen. Only boundary AD is exposed to external conditions, which are on one hand constant relative humidity of 60 % and 20°C temperature, and on the other hand an atmospheric oxygen concentration of 0.25 mol/m³. To prevent any rigid body motion, the horizontal displacement is set to zero on boundary BC.

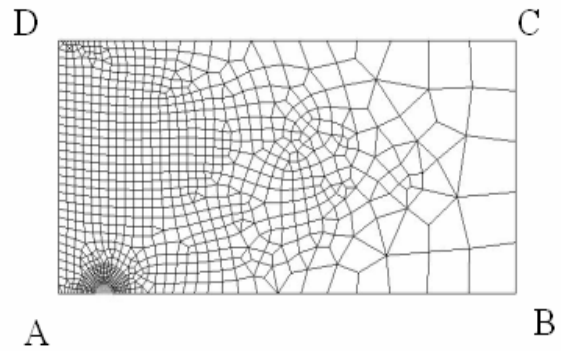


Figure 2. Mesh of the half slab (symmetry axis along AB).

The initial conditions correspond to a saturation degree of 95 % in the concrete as well as in the rust, and a zero oxygen concentration. This latter value has been adopted by defect, but it is most probably not realistic. Nevertheless, it will mostly influence the initial transient period, which is not so important for the corrosion long term process. This point has been checked on the following application, on a reinforced concrete beam.

The steel has a linear elastic isotropic behaviour, with a Young's modulus of 210 GPa, and a Poisson's ratio 0.3. The rust is also considered as a linear elastic material, with a Young's modulus of 9 GPa. For the concrete, the Mazars' isotropic damage model (Mazars 1984) is used with the following parameters: Young's modulus 32 GPa, Poisson's ratio 0.2, traction strength 4.7 MPa, compression strength 42.3 MPa.. Concerning the transport properties, the concrete has a water/cement ratio of 0.4 (leading to $K = 1.2 \cdot 10^{-8}$ m²/s, and $n = 0.23$), a porosity of 15 %, an intrinsic permeability of 10^{-21} m². Finally, the reaction kinetic constant is 10^{-5} m/s, and the coefficient of expansion of the rust is 4. These parameters have been chosen for the present exercise, without trying to identify them from a real test case.

3.2 Results

Two different concrete cover values have been investigated, a low one equal to 3 cm, and a large one equal to 6 cm. The evolution of the cracks pattern induced by the growth of the corrosion products layer has been compared. Here, the cracks correspond to a damage parameter equal to 1. The results tend to confirm the experimental observations already done by Nguyen (2007), although the tests conditions are different: in Nguyen's experiments, the corrosion being induced by a prescribed electrical current together with addition of chlorides to the water, which results in a more or less uniform corrosion products layer around the rebar, while in the present simulation, the corrosion is due to atmospheric conditions applied only on one side of the sample, which results in a non uniform corrosion

rate and by the way, a non uniform corrosion products layer.

Nevertheless, in both cases, the cracks initiate around the rebar. Then, for a small concrete cover a through crack forms along the symmetry line, starting from the outer boundary (Fig. 2 top). On the contrary, for a large concrete cover, two inclined through cracks are formed, leading to a concrete spalling (Fig. 2 bottom). Note that in these figures, the times corresponding to cracks formation are not necessarily the same.

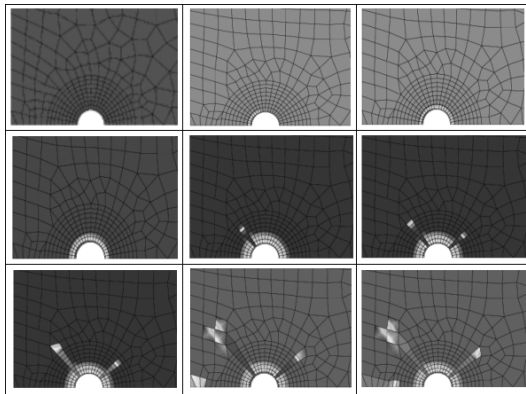


Figure 3. Evolution of the cracks pattern with time. Top: 3 cm concrete cover, bottom: 6 cm concrete cover.

Some other sensitivity analyses have been conducted on the concrete Young's modulus and the coefficient of expansion of the rust.

In these calculations, it appears clearly that the mesh should be refined to better capture the cracks propagation stage, but the main goal here was rather to demonstrate the possibilities of the model. Its applicability to a three-dimensional structure will be the subject of the next paragraph.

4 CORROSION OF A BEAM UNDER 3 POINTS BENDING LOAD

4.1 Studied beam and model set-up

As in the bi-dimensional case, an hypothetical structure has been inspired from real experiments performed at LMDC (Castel et al. 2007) since 1984,

which consisted in subjecting reinforced concrete beams to a maintained three points bending load, and to cyclic chloride environmental conditions. The beam which is considered here is 3m long, with a cross-section of 28cmx15cm. The concrete cover is 4 cm. The details of the reinforcements are shown on Figure 3.

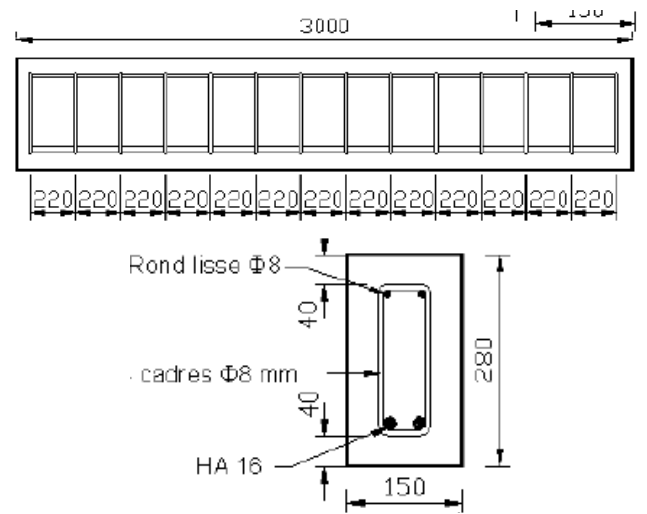


Figure 4. Beam dimensions and reinforcements.

The beam is simply supported at its two ends, and the applied loading generates a constant bending moment of 13,5 kNm in the centre of the beam, corresponding to a service load. In order to apply the atmospheric corrosion model to this structure, it has been decided to use the same material properties as for the bi-dimensional slab, as well as the same environmental conditions. Moreover, only the upper and lower faces of the beam are supposed to be exposed to drying and oxygen penetration.

Thanks to the two symmetry planes of the beam, only one quarter of it needs to be meshed.

4.2 Results under pure bending load

Under the 3 points bending load, some cracks are formed in the central part of the beam, at the locations of the stirrups (Fig. 4). The steel-concrete interface is degraded along the stirrups as well as the lower longitudinal rebar.

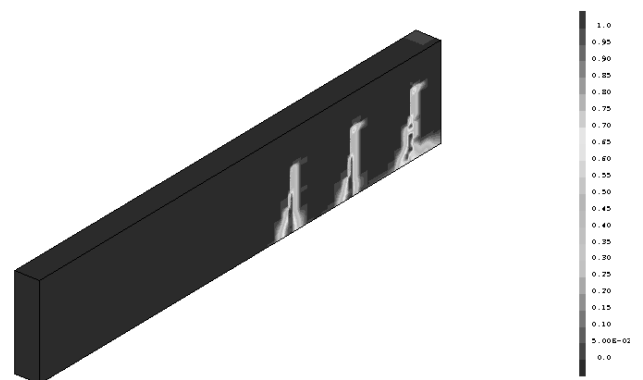


Figure 5. Cracks pattern under 3 points bending load.

4.3 Results under combined bending load and corrosion

While maintaining the bending load, the beam is subjected to corrosion for 50 years. The simultaneous evolutions of the saturation degree, oxygen concentration and mechanical degradation are computed over this period.

Concerning the saturation degree, in the first days, very steep gradients form close to the top and bottom surfaces of the beam, because of the very low intrinsic permeability of the concrete. These gradients diminish slowly with time. After 50 years, the saturation degree is not yet homogeneous in the beam: it is equal to 0.35 (value which corresponds to the prescribed outer relative humidity of 60%) close to the top and bottom surfaces, whereas in the mid layer, it is close to 0.55.

As outlined before, the saturation degree influences the oxygen concentration through the diffusivity coefficient. The oxygen concentration distribution is controlled on one hand by the reaction rate at the interface between the concrete and the rebars, and on the other hand by the diffusion rate through the concrete. The figure 5 shows the oxygen concentration distribution after 1 year.

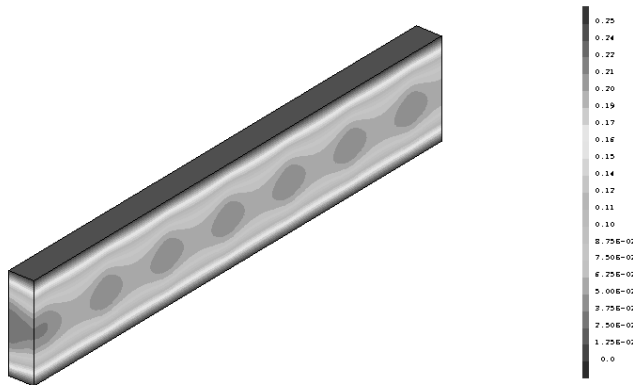


Figure 6. Oxygen concentration distribution after 1 year.

It appears that the consumption of the oxygen by the reaction leads rapidly, in a few tens of days, to the formation of a gradient on the beam height. Moreover, the presence of the stirrups induces more intense oxygen sinks, clearly visible on figure 5. Over the years, this gradient slowly evolves, at the rate of the diffusional process, towards a stationary state which not yet reached after 50 years (Fig 6). Note that the scales on figures 5 and 6 are the same.

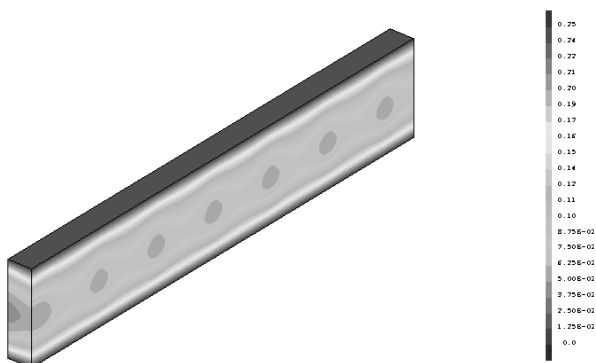


Figure 7. Oxygen concentration distribution after 50 years.

In these calculations, contrary to the slab example, the initial oxygen concentration in the concrete has been taken equal to the atmospheric one. To evaluate the influence of this condition, an additional calculation has been performed starting from a zero oxygen concentration, and the results differ only during the first 50 days.

Concerning the concrete degradation, the growth of the corrosion products leads to an additional damage, which is first, in agreement with the previous results on the slab, distributed along the rebars, but invisible from outside. A new visible crack along a stirrup can be seen at 25 years (Fig. 7) which may be due to the growth of the degradation of the steel concrete interface, causing a stress redistribution in the beam.

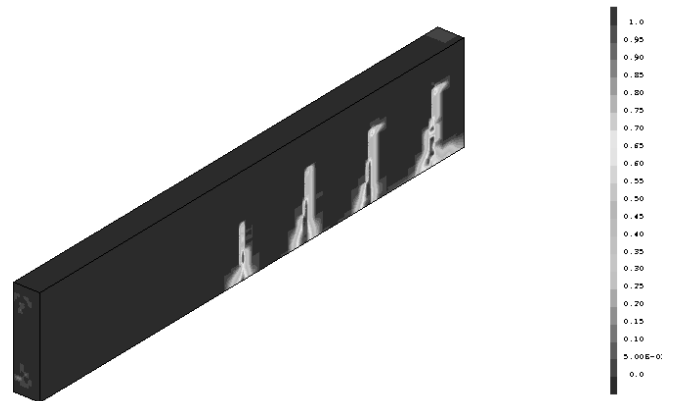


Figure 8. Cracks pattern after 25 years.

Finally, after 50 years of corrosion, many corrosion through-cracks are visible on the beam, following the rebars as it is the case on real corroded beams (Fig. 8).

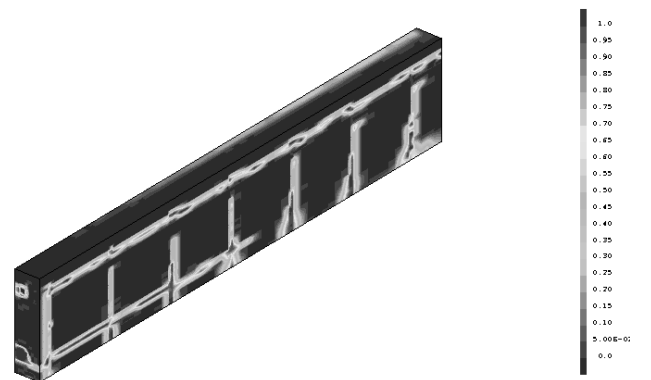


Figure 9. Cracks pattern after 50 years.

4.4 Influence of variable environmental conditions

In the previous calculation, the outer relative humidity and temperature have been kept constant for 50 years, respectively equal to 60% and 20°C. To be more realistic, yearly cyclic conditions have been next considered as follows: keeping the same mean values, a minimum 30% relative humidity and a

maximum 35°C temperature are supposed to be reached in summer, while a maximum 90% relative humidity and a minimum 5°C temperature are reached in winter. It must be noted that the temperature variations are not used for a thermal analysis, but they are solely used in conjunction with the relative humidity in Kelvin's law to derive the corresponding capillary pressure.

Because of the variable outer conditions, the saturation degree follows a more complex and slower decreasing evolution. The cycles lead, after 50 years, to a value in the mid layer of the beam of 0.62 instead of 0.55. This difference can be explained by the fact that, although the cycles are symmetrical with respect to the mean values, the relative water permeability is larger for the wetting phases than for the drying phases, thus leading to a resaturation faster than the desaturation.

The consequence on the oxygen concentration is a reduction, because of the lower diffusion coefficient for a higher saturation degree. Finally, the corrosion rate is also lower, which leads to a slower corrosion induced degradation of the beam. This can be seen on figures 9 and 10, where the crack pattern obtained after 25 years does not yet show any visible effect of corrosion, while the crack pattern after 50 years of cyclic environmental conditions is comparable to the one obtained after 25 years under constant conditions.

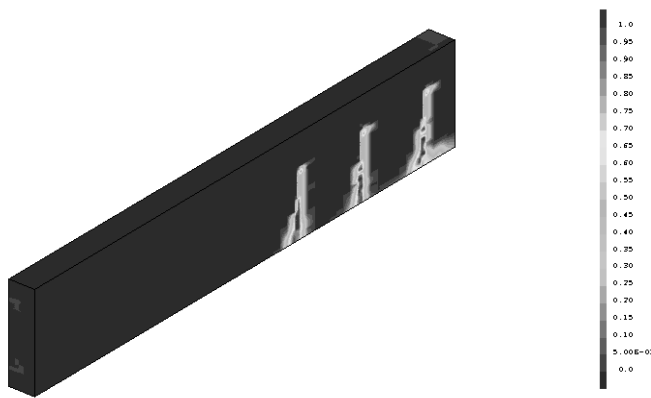


Figure 10. Cracks pattern after 25 years, under cyclic environmental conditions.

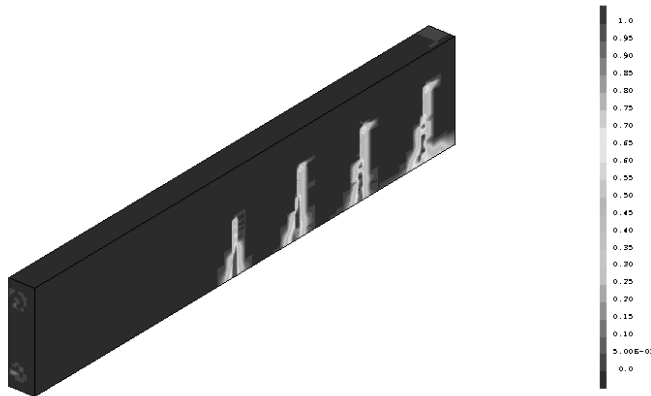


Figure 11. Cracks pattern after 50 years, under cyclic environmental conditions.

5 CONCLUSION

In this paper, an atmospheric corrosion model has been presented and applied to simple bi-dimensional and three-dimensional cases. Compared to previous approaches, it has been possible to predict the corrosion rate, starting with the onset of active corrosion phase, and then the development of damage up to visible cracks formation.

The first application to a specific slab, containing a rebar cross-section, was made to check the ability of the model to reproduce experimentally observed cracks patterns.

The second application to a reinforced concrete beam was done to demonstrate the potentialities of the model to predict the long term degradation of a structure subjected to atmospheric corrosion. The predicted cracks pattern induced by corrosion shows similarities with usual observations on corroded structures. Moreover, the influence of more realistic cyclic environmental conditions has been investigated. Of evidence, after these preliminary studies, an in-depth validation has to be done.

Additional developments of the model are in progress, including :

- an experimental determination of the mechanical and transport properties of the rust,
- accounting for the degradation of the concrete-rebar bond by corrosion,
- accounting for the changes of transport properties induced by damage.

Moreover, in order to be able to make full predictions of the life-time of a structure, it will be necessary to model the passive corrosion phase, up to the depassivation of the rebars.

ACKNOWLEDGEMENTS

This study has been financially supported by CEA and Electricité de France with the CIMETAL research program. The support of the French National Research Agency, in the framework of the APPLLET project, is also gratefully acknowledged.

REFERENCES

- Castel A., Vidal T., Zhang R. 2007 Corrosion initiation and propagation in the service life of reinforced concrete in chloride environment *International RILEM Workshop on Integral Service Life Modeling of Concrete Structures Portugal*
- Chitty W.J., Dillmann P., L'Hostis V. & Millard A. 2008 Use of ferrous archaeological artefacts as analogous systems and feedback tools for rebars embedded in concrete – An analytical corrosion modelling *Corrosion Science* 50: 3047-3055

- Huet B., L'Hostis V., Miserque F. & Idrissi H. 2005 Electrochemical behaviour of mild steel in concrete: influence of pH and carbonate content of concrete pore solution *Electrochimica Acta* 51 (1):172-180
- L'Hostis, V., Foct F. & Dillmann, P. 2008. Corrosion behaviour of reinforced concrete: Laboratory experiments and archaeological analogues for long-term predictive modelling *Journal of Nuclear Materials* 379:124-132
- Mazars J. 1984 Application de la mécanique de l'endommagement au comportement non linéaire et à la rupture du béton de structure *Phd Thesis* Paris
- Millard A., Beddiar K., Berthaud Y. & L'Hostis V. 2004 Modelling the cracking of a reinforced concrete structure submitted to corrosion of steels- First validation of a damage model based on experimental results *CSNI/Rilem Workshop on use and performance of concrete in NPP fuel cycle facilities* Madrid
- Nguyen Q.T., Millard A., Caré S., L'Hostis V. & Berthaud Y. 2006 Fracture of concrete caused by the reinforcement corrosion products *Journal de Physique IV*
- Nguyen Q. T., Caré S., Millard A. & Berthaud Y. 2007 Analyse de la fissuration du béton armé en corrosion accélérée *C.R. Mécanique* 335 : 99-104
- Papadakis V.G., Vayenas C.G. & Fardis M.N. 1991 Fundamental concrete carbonation model and application to durability of reinforced concrete. In Baker, J.M., Nixon, P.J., Majumdar, A.J. & Davies H. *Durability of building materials and components*: 27-38.
- Van Genuchten M. 1980 A closed-form equation for predicting the hydraulic conductivity of unsaturated soils *Soils science society of America* 44: 892-898
- Verpeaux P., Millard A., Charras T. & Combescure A., 1989 A modern approach of large computer codes for structural analysis *Proc SMiRT 10*, Los Angeles